AAS 13-292

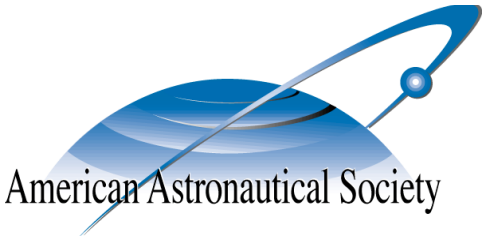

American Institute of
Aeronautics and Astronautics

THREE-AXIS ATTITUDE CONTROL USING REDUNDANT REACTION WHEELS WITH CONTINUOUS MOMENTUM DUMPING

Erik A. Hogan, and Hanspeter Schaub

AAS/AIAA Spaceflight Mechanics Meeting

Kauai, Hawaii **February 10–14, 2013**

AAS Publications Office, P.O. Box 28130, San Diego, CA 92198

AAS 13-292

THREE-AXIS ATTITUDE CONTROL USING REDUNDANT REACTION WHEELS WITH CONTINUOUS MOMENTUM DUMPING

Erik A. Hogan[*] **and Hanspeter Schaub**[†]

A description of an attitude control system for a 3-axis stabilized spacecraft is presented. Using modified Rodrigues parameters, a globally stabilizing nonlinear feedback control law is derived that enables tracking of an arbitrary, time-varying reference attitude. This new control incorporates integral feedback while avoiding any quadratic rate feedback components. A redundant cluster of four reaction wheels is used to control the spacecraft attitude, and three magnetic torque rods are used for purposes of continuous autonomous momentum dumping. The momentum dumping strategy can employ general torque rod orientations, and is developed to take advantage of a redundant set of reaction wheels.

INTRODUCTION

The use of momentum exchange devices, such as reaction wheels, is a common method of spacecraft attitude control. Such devices work through momentum transfer between the spacecraft body and one or more spinning wheels. To detumble a spacecraft, wheel speeds are modified in such a way as to effectively absorb the spacecraft momentum. The same principle may be used by a cluster of reaction wheels for arbitrary three-axis spacecraft pointing. Here, motor torques drive wheel accelerations; these motor torques, in turn, act equally and opposite on the spacecraft frame. By carefully controlling the wheel accelerations, torque is created which allows for general attitude corrections.[1,2,3,4] Due to the interface between the reaction wheel assemblies and the spacecraft, the total momentum of the system is constant. The limitation of reaction wheels actuation is the speed to which a fly-wheel can be accelerated before. This saturation can lead to stability or performance concerns. Thus, it is desirable for a reaction wheel control law to avoid saturation if feasible.

A practical consideration with the use of reaction wheels is the need for momentum dumping.[5,6] Because the system of spacecraft and reaction wheels conserves momentum, as the spacecraft loses momentum the wheel speeds must increase. Additionally, any perturbing torques acting on the spacecraft must be absorbed by the wheels if precise pointing is to be maintained. Due to the inherent size and speed limitations of physical systems, wheel speeds may become saturated after a period of time, preventing further attitude control of the spacecraft. If the momentum storage capacity of the reaction wheel cluster is not large enough to absorb all of the spacecraft momentum the wheel speeds reach their maximum values and further wheel acceleration is not possible. A method of torquing the spacecraft besides the reaction wheels is needed in order to despin the wheels while still meeting the attitude control requirements. One method for accomplishing this

[*]Graduate Student, Laboratory for Atmospheric and Space Physics, University of Colorado, Boulder, CO.
[†]Associate Professor, H. Joseph Smead Fellow, Aerospace Engineering Sciences, University of Colorado, Chief Technologist, Wacari Group, Boulder, CO

task is the use of thrusters.[7] By angling the thrusters off-center from the spacecraft center-of-mass, torques are created that can be used to lower wheel speeds.

Another option for momentum dumping is the use of magnetic torque rods.[5,8,9] Here, coils of wire are wrapped around a ferrous core, such as iron. Applying a current to the wire produces a magnetic dipole that, in turn, interacts with the earth's magnetic field to produce a torque on the spacecraft. This torque is then used to despin the wheels. A challenge with using magnetic torque rods lies in their inability to produce an arbitrary three-dimensional torque. In fact, a torque can only be produced perpendicular to the earth's magnetic field, providing only two degrees of freedom available for dumping wheel momentum.[10,11]

In this paper, an autonomous control is presented for a three-axis stabilized spacecraft . This pointing control is achieved using a redundant combination of four reaction wheels for attitude control and three magnetic torque rods for momentum dumping. However, the methodology developed is general enough to be applicable for an arbitrary number of redundant reaction wheels and magnetic torque bars. The control algorithm is parameterized using modified Rodrigues parameters (MRPs) as the attitude description,[12,13,14,15] and a nonlinear feedback control law capable of tracking a time-varying arbitrary attitude is developed. A new MRP-based feedback control is developed for a spacecraft with a redundant set of reaction wheels that still guarantees global asymptotic stability, but includes an integral error measure while avoiding quadratic rate feedback terms. The integral feedback provides robustness to unmodeled disturbance torques. This combination of integral feedback while avoiding quadratic angular velocity feedback components is a new development that helps avoid control saturation issues when handling initial detumbling after being released from the launch vehicle.

The redundancy of having four reaction wheels presents a challenge for momentum dumping. For any desired torque, there are an infinite number of wheel accelerations that may be used to achieve it. If a magnetic torque is created for momentum dumping purposes, a solution for the motor torques must be chosen to offset it such that the wheels actually spin down. There is no guarantee that any arbitrary solution will not further increase wheels speeds, leading to wheel saturation. To that end, a momentum dumping strategy is investigated for the case of a redundant reaction wheel cluster. The solution should be very general in that the reaction wheels and torque rod actuation axes can have general body-fixed orientations. This more general solution should provide effective autonomous momentum dumping, and integrate well with the attitude control law. If the reaction wheel cluster is redundant, the momentum dumping strategy is desired to exploit the reaction wheel nullspace. The end-result should be a single strategy for general configurations.

The paper is structured as follows. First, background information is provided regarding the dynamics of a spacecraft equipped with reaction wheels and magnetic torque bars. Next, Lyapunov stability theory is used to derive a globally stabilizing attitude control law. A novel momentum dumping strategy is developed, following a discussion on the limitations of current methods for redundant systems. Lastly, a numerical simulation is used to demonstrate both the attitude control law and momentum dumping strategy.

BACKGROUND

Rotational Equations of Motion

In this paper, a rigid body spacecraft outfitted with a redundant set of reaction wheels ($n > 3$) and a set of magnetic torque bars is considered, as depicted in Figure 1. While four reaction wheels

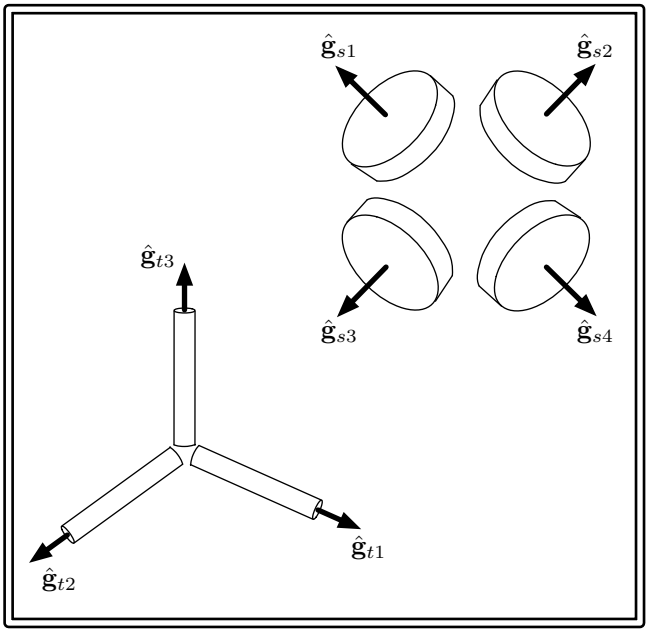

Figure 1. Illustration of spacecraft with redundant reaction wheels and magnetic torque bars.

and three torque bars are shown, the developments in this paper are formulated in a general way that can account for different numbers of these actuation devices. The primary function of the reaction wheels is to provide three-axis pointing. Due to the process of momentum exchange between the wheels and spacecraft, a method for dumping momentum is needed. As momentum accrues in the reaction wheel cluster, the wheel speeds will increase to a point where further actuation is severely hindered.[5] To that end, a set of magnetic torque bars is used for the purpose of momentum dumping. The magnetic torque bars work by creating a torque on the spacecraft due to their interaction with the earth's magnetic field. For a single torque bar, the resulting torque is[16]

$$\boldsymbol{\tau}_{TBi} = \mu_i \hat{\boldsymbol{g}}_{ti} \times \boldsymbol{B},$$

where μ_i is the strength of the magnetic dipole of the torque bar, $\hat{\boldsymbol{g}}_{ti}$ is the alignment axis of the torque bar, and $\boldsymbol{B}$ is the earth's magnetic field. It is important to note that a magnetic torque bar is only capable of producing torque in the plane perpendicular to the magnetic field. For the full set of N torque bars, the resulting torque on the spacecraft is expressed as

$$\boldsymbol{\tau}_{TB} = -[\tilde{\boldsymbol{B}}][G_t]\boldsymbol{\mu}, \tag{1}$$

where $[\tilde{\boldsymbol{B}}]$ denotes the skew-symmetric matrix, $[G_t] = [\hat{\boldsymbol{g}}_{t1}\ \hat{\boldsymbol{g}}_{t2}\ ...\ \hat{\boldsymbol{g}}_{tN}]$, and $\boldsymbol{\mu} = [\mu_1\ \mu_2\ ...\ \mu_N]^T$.

As depicted in Figure 1, the spin-axis of each reaction wheel is denoted as $\hat{\boldsymbol{g}}_{si}$. The momentum exchange between spacecraft and wheels is accomplished through careful application of motor torques u_{si}. These torques, in turn, act to change the wheel speeds, which are defined relative to the spacecraft and referred to as Ω_i. Thus, the momentum of a single wheel about its spin axis is

$$h_i = J_{si}(\Omega_i + \hat{\boldsymbol{g}}_{si}^T \boldsymbol{\omega}), \tag{2}$$

where J_{si} is the inertia of the wheel about its spin axis and $\boldsymbol{\omega}$ is the spacecraft angular velocity. In accordance with Euler's equation, the wheel speeds evolve as a result of applied motor torques according to

$$u_{si} = J_{si}(\dot{\Omega} + \hat{\boldsymbol{g}}_{si}^T \dot{\boldsymbol{\omega}}). \tag{3}$$

The rotational motion of a spacecraft equipped with n reaction wheels and N magnetic torque bars is described by[3]

$$[I]\dot{\boldsymbol{\omega}} = -\boldsymbol{\omega} \times ([I]\boldsymbol{\omega} + [G_s]\boldsymbol{h}_s) - [G_s]\boldsymbol{u}_s - [\tilde{\boldsymbol{B}}][G_t]\boldsymbol{\mu} + \boldsymbol{L}, \tag{4}$$

where $[I]$ is the inertia tensor of the spacecraft, and

$$[G_s] = [\hat{\boldsymbol{g}}_{s1}\ \hat{\boldsymbol{g}}_{s2}\ ...\ \hat{\boldsymbol{g}}_{sn}] \tag{5a}$$

$$\boldsymbol{h}_s = [h_1\ h_2\ ...\ h_n]^T \tag{5b}$$

$$\boldsymbol{u}_s = [u_1\ u_2\ ...\ u_n]^T \tag{5c}$$

while $\boldsymbol{L}$ is the external torque acting on the spacecraft.

Modified Rodrigues Parameters

In order to perform attitude control maneuvers, some measure of attitude is required. In the current study, the modified Rodrigues parameter (MRP) set is used.[17,18,19] The MRP set is constructed from the principle rotation vector attitude description as[3]

$$\boldsymbol{\sigma} = \tan\left(\frac{\Phi}{4}\right)\hat{\boldsymbol{e}}, \tag{6}$$

where Φ is the principle rotation angle and $\hat{\boldsymbol{e}}$ is the principle rotation vector. The MRP set is a minimal attitude description. That is, three coordinates are used to describe a three-dimensional rotation. As such, singularities are present in the description. Examination of Eq. (6) reveals that the description is singular when $\Phi = \pm 360^\circ$.

Fortunately, this singularity may be avoided by switching to the shadow MRP set. Indeed, for any given attitude there are two different sets of modified Rodrigues parameters that describe it. The mapping between original and shadow set is[3]

$$\sigma_i^S = -\frac{\sigma_i}{\sigma^2}, \tag{7}$$

where the superscript S is used to denote the shadow set and $\sigma^2 = \boldsymbol{\sigma}^T\boldsymbol{\sigma}$. It is clear that as the original MRP set approaches the singularity, its corresponding shadow set approaches 0. Thus, the inherit singularities present with modified Rodrigues parameters can be avoided by switching to the shadow set. The location of this switching is arbitrary, and switching is typically performed when the norm of the MRP set exceeds a value of 1. Switching in this manner guarantees the attitude description will be well defined for all orientations.

The kinematic differential equation for the MRP set is[13]

$$\dot{\boldsymbol{\sigma}} = \frac{1}{4}\left[(1-\sigma^2)\mathbb{I} + 2[\tilde{\boldsymbol{\sigma}}] + 2\boldsymbol{\sigma}\boldsymbol{\sigma}^T\right]\boldsymbol{\omega}, \tag{8}$$

where $\mathbb{I}$ is the 3×3 identity matrix. Note that this differential equation holds for both the original and shadow set of the modified Rodrigues parameters. Combined with Eqs. (3) and (4), Eq. (8) describes the full attitude motion of the spacecraft.

ATTITUDE CONTROL

Nonlinear Attitude Control Law

The tracking problem of an arbitrary, possibly time-varying reference attitude is considered. Let the reference frame be denoted as $\mathcal{R}$. The goal of the attitude tracking control law is to reorient the spacecraft body frame, $\mathcal{B}$, such that it matches $\mathcal{R}$. The attitude error between $\mathcal{B}$ and $\mathcal{R}$ is described using the MRP description $\boldsymbol{\sigma}$. It follows, then, that by driving $\boldsymbol{\sigma} \to \mathbf{0}$, attitude tracking is achieved. Furthermore, if the reference attitude is time-varying then the spacecraft angular velocity, $\boldsymbol{\omega}$, must track that of the reference frame, $\boldsymbol{\omega}_r$.

Consider the candidate Lyapunov function

$$V(\boldsymbol{\sigma}, \delta\boldsymbol{\omega}, \boldsymbol{z}) = \frac{1}{2}\delta\boldsymbol{\omega}^T[I]\delta\boldsymbol{\omega} + 2K\ln(1+\boldsymbol{\sigma}^T\boldsymbol{\sigma}) + \frac{1}{2}\boldsymbol{z}^T[K_I]\boldsymbol{z}, \tag{9}$$

where $\delta\boldsymbol{\omega} = \boldsymbol{\omega} - \boldsymbol{\omega}_r$, K is a scalar gain, $[K_I]$ is a gain matrix, and $\boldsymbol{z}$ is the integral term[3,20]

$$\boldsymbol{z} = \int_0^t \left(K\boldsymbol{\sigma} + [I]\delta\dot{\boldsymbol{\omega}}\right) dt. \tag{10}$$

This integral term is added to provide robustness in the presence of unmodeled external torques. The Lyapunov function is positive definite about $\boldsymbol{\sigma} = \mathbf{0},\ \boldsymbol{\omega} = \boldsymbol{\omega}_r,\ \boldsymbol{z} = \mathbf{0}$. Computing the derivative of the Lyapunov function yields

$$\dot{V}(\boldsymbol{\sigma}, \delta\boldsymbol{\omega}, \boldsymbol{z}) = \left(\delta\boldsymbol{\omega} + [K_I]\boldsymbol{z}\right)^T \left([I]\dot{\boldsymbol{\omega}} - [I]\left(\dot{\boldsymbol{\omega}}_r - \boldsymbol{\omega}\times\boldsymbol{\omega}_r\right) + K\boldsymbol{\sigma}\right). \tag{11}$$

Plugging in Eq. (4), the Lyapunov rate becomes

$$\dot{V}(\boldsymbol{\sigma}, \delta\boldsymbol{\omega}, \boldsymbol{z}) = \Big(\delta\boldsymbol{\omega} + [K_I]\boldsymbol{z}\Big)^T \Big(-\boldsymbol{\omega}\times\left([I]\boldsymbol{\omega} + [G_s]\boldsymbol{h}_s\right) - [G_s]\boldsymbol{u}_s + \boldsymbol{L} - [I]\left(\dot{\boldsymbol{\omega}}_r - \boldsymbol{\omega}\times\boldsymbol{\omega}_r\right) + K\boldsymbol{\sigma}\Big). \tag{12}$$

Note that the magnetic torque has been omitted in this development. It is considered in the following section regarding momentum dumping. Its omission does not impact the stability guarantees derived here.

To ensure Lyapunov stability, the motor torques $\boldsymbol{u}_s$ are employed to cause the Lyapunov rate to take the negative semi-definite form

$$\dot{V}(\boldsymbol{\sigma}, \delta\boldsymbol{\omega}, \boldsymbol{z}) = -(\delta\boldsymbol{\omega} + [K_I]\boldsymbol{z})^T[P](\delta\boldsymbol{\omega} + [K_I]\boldsymbol{z}), \tag{13}$$

where $[P]$ is a positive definite gain matrix. In prior work,[3] this is accomplished by directly compensating the natural dynamics present in Eq. (12). Such an approach yields a control law of

$$[G_s]\boldsymbol{u}_s = -[I]\left(\dot{\boldsymbol{\omega}}_r - \boldsymbol{\omega}\times\boldsymbol{\omega}_r\right) + K\boldsymbol{\sigma} + [P]\delta\boldsymbol{\omega} + [P][K_I]\boldsymbol{z} - \boldsymbol{\omega}\times\left([I]\boldsymbol{\omega} + [G_s]\boldsymbol{h}_s\right) + \boldsymbol{L}. \tag{14}$$

While this solution achieves the desired negative semi-definite form and can be shown to be asymptotically stabilizing, it suffers from the presence of the quadratic angular velocity term $-\boldsymbol{\omega}\times[I]\boldsymbol{\omega}$. If the angular velocity is high, this quadratic term can become large enough to lead to control saturation, invalidating the analytic stability guarantees.

In the current paper, we present a novel control formulation that eliminates the need for this quadratic term while still providing asymptotic stability. Consider the control law

$$[G_s]\boldsymbol{u}_s = -[I](\dot{\boldsymbol{\omega}}_r - \boldsymbol{\omega}\times\boldsymbol{\omega}_r) + K\boldsymbol{\sigma} + [P]\delta\boldsymbol{\omega} + [P][K_I]\boldsymbol{z} - (\widetilde{[\boldsymbol{\omega}_r]} - \widetilde{[K_I]\boldsymbol{z}})([I]\boldsymbol{\omega} + [G_s]\boldsymbol{h}_s) + \boldsymbol{L}, \tag{15}$$

where the over tilde is used to denote the skew-symmetric matrix. Substituting this into Eq. (12) yields

$$\dot{V}(\boldsymbol{\sigma}, \delta\boldsymbol{\omega}, \boldsymbol{z}) = (\delta\boldsymbol{\omega} + [K_I]\boldsymbol{z})^T\Big[(-\widetilde{[\delta\boldsymbol{\omega}]} - \widetilde{[K_I]\boldsymbol{z}})([I]\boldsymbol{\omega} + [G_s]\boldsymbol{h}_s) - [P]\delta\boldsymbol{\omega} - [P][K_I]\boldsymbol{z}\Big]. \tag{16}$$

Noting the identity

$$(\delta\boldsymbol{\omega} + [K_I]\boldsymbol{z})^T\Big(-\widetilde{[\delta\boldsymbol{\omega}]} - \widetilde{[K_I]\boldsymbol{z}}\Big)\Big([I]\boldsymbol{\omega} + [G_s]\boldsymbol{h}_s\Big) = 0,$$

the Lyapunov rate reduces to the negative semi-definite form in Eq. (13). Thus, the system will converge to the set $\delta\boldsymbol{\omega} + [K_I]\boldsymbol{z} = \boldsymbol{0}$.

To determine asymptotic stability, higher order derivatives of the Lyapunov function are evaluated on the set $\delta\boldsymbol{\omega} + [K_I]\boldsymbol{z} = \boldsymbol{0}$.[21] The second derivative is identically zero ($\ddot{V} = 0$) and the third derivative reduces to

$$\dddot{V}(\boldsymbol{\sigma}, \delta\boldsymbol{\omega}, \boldsymbol{z}) = -2K^2\boldsymbol{\sigma}^T[I]^{-1}[P][I]^{-1}\boldsymbol{\sigma}, \tag{17}$$

which is negative definite. Thus, the control law is asymptotically stabilizing, i.e. $\boldsymbol{\sigma} \to \boldsymbol{0}$. Furthermore, the kinematic coupling between the MRP set and the angular velocity guarantees that if $\boldsymbol{\sigma}$ converges to $\boldsymbol{0}$, then $\delta\boldsymbol{\omega}$ must also converge to zero. Lastly, the integral term $\boldsymbol{z}$ must converge to $\boldsymbol{0}$ to satisfy $\delta\boldsymbol{\omega} + [K_I]\boldsymbol{z} = \boldsymbol{0}$.

The new control law in Eq. (15) does not contain a quadratic function of $\boldsymbol{\omega}$. It does however, contain a term proportional to $\boldsymbol{\omega}\times\boldsymbol{\omega}_r$. In general, $\boldsymbol{\omega}_r$ will not be large enough to be problematic. In order to compute the necessary motor torques, the $[G_s]$ matrix must be inverted. In a redundant system, this matrix will be of dimension $3 \times n$ and a minimum norm inverse may be used.

The integral term $\boldsymbol{z}$ is included to provide robustness in the presence of unmodeled torques. A torque that is not accounted for will cause the Lyapunov rate to lose its negative semi-definiteness. Instead, the Lyapunov rate will be

$$\dot{V}(\boldsymbol{\sigma}, \delta\boldsymbol{\omega}, \boldsymbol{z}) = -(\delta\boldsymbol{\omega} + [K_I]\boldsymbol{z})^T([P](\delta\boldsymbol{\omega} + [K_I]\boldsymbol{z}) - \Delta\boldsymbol{L}), \tag{18}$$

where $\Delta\boldsymbol{L}$ is the unmodeled torque. Though the stability guarantees no longer hold, $\delta\boldsymbol{\omega}$ and $\boldsymbol{z}$ cannot grow unbounded because the quadratic $(\delta\boldsymbol{\omega}+[K_I]\boldsymbol{z})^T[P](\delta\boldsymbol{\omega}+[K_I]\boldsymbol{z})$ term will eventually dominate, making $\dot{V}$ negative. If $\boldsymbol{\sigma}$ did not converge to $\boldsymbol{0}$, then the integral term $\boldsymbol{z}$ would grow unbounded. Therefore, $\boldsymbol{\sigma}$ must converge to $\boldsymbol{0}$, along with $\delta\boldsymbol{\omega}$. So, asymptotic stability still holds for the attitude, but the integral term will no longer converge to $\boldsymbol{0}$. For further discussion on this matter, the reader is referred to Reference 3.

Momentum Dumping Strategy

As the wheels are spun up to provide attitude control they will eventually reach their saturation limit with regards to wheel speeds if left unchecked. To eliminate momentum from the spacecraft/reaction wheel system, an external means of torquing is required. The magnetic torque bars

are used for this purpose. By creating a magnetic torque on the spacecraft in a controlled manner and compensating for it with the reaction wheels, the wheels can be despun while simultaneously achieving attitude control.

In prior work,[5,8,9] a cross product desaturation control law is used. The magnetic dipole produced by the torque bars is proportional to

$$\boldsymbol{\mu} \sim \Delta \boldsymbol{h} \times \boldsymbol{B}, \tag{19}$$

where $\Delta \boldsymbol{h} = \boldsymbol{h}_W - \boldsymbol{h}_B$. At any given time, the angular momentum vector of the reaction wheels, $\boldsymbol{h}_W$, is given by

$$\boldsymbol{h}_W = [G_s]\boldsymbol{h}_s.$$

In practice, reaction wheels are often biased towards non-zero wheel speeds. These non-zero wheels speeds result in a desired bias angular momentum, $\boldsymbol{h}_B$. In the case of three reaction wheels, this strategy is sufficient, as a non-zero $\Delta \boldsymbol{h}$ vector implies the wheel speeds are not biased properly.

In a redundant system, however, such a formulation can be problematic. This is due to the fact that the set of four or more reaction wheels span a three-dimensional space in a manner that allows for non-unique control solutions. For example, for a necessary torque there are an infinite number of motor torques that may be used to achieve it. Similarly, there are an infinite number of wheel speeds that may result in a given $\boldsymbol{h}_W$. Thus $\Delta \boldsymbol{h}$ may be $\mathbf{0}$, or very small, even for large wheel speeds. In such a scenario, the resulting desaturation magnetic torque would be virtually nonexistent in spite of the fact that the wheels are nowhere near the desired bias.

To prevent these issues, a method for handling desaturation in a redundant system is developed. First, note that the motor torque equation may be approximated by

$$\boldsymbol{u}_s = [J_s]\dot{\boldsymbol{\Omega}}, \tag{20}$$

where $[J_s] = \text{diag}([J_{s1}\ J_{s2}\ ...\ J_{sn}])$ and $\dot{\boldsymbol{\Omega}} = [\dot{\Omega}_1\ \dot{\Omega}_2\ ...\ \dot{\Omega}_n]^T$. In general, $\dot{\boldsymbol{\omega}}$ will be small and not significantly impact the evolution of the wheel speeds. To impose a despin torque on each wheel, a feedback on wheel speeds is used

$$\boldsymbol{u}_s^* = -c[J_s](\boldsymbol{\Omega} - \boldsymbol{\Omega}_r), \tag{21}$$

where c is a gain and $\boldsymbol{\Omega}_r$ are the wheel speed biases. Superimposing these desaturation torques on top of the control solution in Eq. (15) results in a net torque on the spacecraft of

$$\boldsymbol{\tau}_{RW} = -[G_s]\boldsymbol{u}_s^*. \tag{22}$$

To counteract this, the magnetic torque bars are used. An attempt is made to perfectly offset the despin torque by controlling the dipoles of the individual magnetic torque bars using

$$-[\tilde{\boldsymbol{B}}][G_t]\boldsymbol{\mu} = [G_s]\boldsymbol{u}_s^*. \tag{23}$$

The torque bars are limited, however, due to the fact that they can only generate torque perpendicular to the magnetic field vector. Generally, the product $[\tilde{\boldsymbol{B}}][G_t]$ is not full rank, and a direct inverse is not possible. Instead, a singular value decomposition (SVD) pseudoinverse is performed.[22] The resulting solution for the dipoles is given by

$$\boldsymbol{\mu}^* = -\left([\tilde{\boldsymbol{B}}][G_t]\right)^{\dagger}[G_s]\boldsymbol{u}_s^*, \tag{24}$$

where the superscript † is used to represent the pseudoinverse. This least-squares-like inverse yields dipoles whose total magnetic torque approximates the desired momentum dumping torque $\boldsymbol{u}_s^*$ the closest.

The resulting magnetic dipoles interact with the earths magnetic field to produce a torque on the spacecraft equivalent to

$$\boldsymbol{\tau}_{MTB} = -[\tilde{\boldsymbol{B}}][G_t]\boldsymbol{\mu}^*. \tag{25}$$

Ideally, $\boldsymbol{\tau}_{RW} + \boldsymbol{\tau}_{MTB} = \mathbf{0}$. However, this will rarely, if ever, be the case due to the inability of the torque bars to generate torque in the direction of the magnetic field. If left unchecked, the resulting imbalance between the desaturation torque $\boldsymbol{\tau}_{RW}$ and the torque bar compensation torque $\boldsymbol{\tau}_{RW}$ will result in a nonzero perturbation on the spacecraft that will drive it away from the desired attitude. A final addition is made to the motor torques to account for this difference, and is computed as

$$\Delta\boldsymbol{u} = [G_s]^+(\boldsymbol{\tau}_{MTB} - [G_s]\boldsymbol{u}_s^*). \tag{26}$$

The superscript $+$ is used to denote a minimum norm inverse. With this correction, the resulting torque acting on the spacecraft due to the desaturation process is zero, i.e.

$$-[G_s](\boldsymbol{u}_s^* + \Delta\boldsymbol{u}) - [\tilde{\boldsymbol{B}}][G_t]\boldsymbol{\mu}^* = \mathbf{0}. \tag{27}$$

The wheel desaturation algorithm is superimposed upon the attitude control solution and does not impact the stability guarantees derived in the previous section due to the net-zero torque it produces. Assuming the control law in Eq. (15) results in a motor torque solution of $\boldsymbol{u}_s = \boldsymbol{L}_r$, the commanded motor torques at any particular time are given by

$$\boldsymbol{u}_s = \boldsymbol{L}_r + \boldsymbol{u}_s^* + \Delta\boldsymbol{u}, \tag{28}$$

with the necessary dipoles computed in Eq. (24). This desaturation strategy may be applied continuously. Furthermore, in the case of $\boldsymbol{h}_W = \boldsymbol{h}_B$ even with large wheel speeds, the desaturation strategy will act to bring the wheels to the desired biases.

Naturally, it is of interest to investigate the possibility that the despin algorithm will actually increase wheel speeds. If the magnetic torque bars were capable of exactly compensating for $\boldsymbol{u}_s^*$, this would not be an issue. Rather, the possibility is due to the fact that a correction motor torque, $\Delta\boldsymbol{u}$, must be added in to compensate for the difference between the despin torques and the realized $\boldsymbol{\tau}_{MTB}$.

Consider the wheel acceleration resulting from the despin torque algorithm

$$[J_s]\dot{\boldsymbol{\Omega}}^* = \boldsymbol{u}_s^* + \Delta\boldsymbol{u}. \tag{29}$$

For the sake of simplicity, an assumption is made that the required attitude pointing motor torque solution $\boldsymbol{L}_r$ is either zero or very small such that it does not significantly impact the wheel accelerations. This would generally occur once pointing has been achieved. Here, we are interested in the longer term evolution of the wheel speeds during the momentum dumping process.

It is possible to derive an equation for the evolution of the wheel speeds during the momentum dumping. Using Eqs. (25) and (26) together with Eq. (29) yields

$$[J_s]\dot{\boldsymbol{\Omega}}^* = \boldsymbol{u}_s^* + [G_s]^+(-[\tilde{\boldsymbol{B}}][G_t]\boldsymbol{\mu}^* - [G_s]\boldsymbol{u}_s^*). \tag{30}$$

Table 1. Orbital parameters used in numerical simulation

a	e	i	Ω	ω	ν_0 (True Anomaly)
6778.14 km	0	45°	60°	0°	0°

Table 2. Control gains used for numerical simulation

$[K]$	$[P]$	$[K_I]$	c
$0.148[\mathbb{I}_{3\times3}]$ Nm	$0.9[\mathbb{I}_{3\times3}]$ Nms	$0.0001[\mathbb{I}_{3\times3}]$ $\text{N}^{-1}\text{s}^{-2}$	0.005 s^{-1}

Substituting in the definitions of $\boldsymbol{\mu}^*$ and $\boldsymbol{u}_s^*$ leads to the non-autonomous linear system

$$\dot{\boldsymbol{\Omega}}^* = -c\left[\mathbb{I} + [G_s]^+\left([\tilde{\boldsymbol{B}}][G_t]\left([\tilde{\boldsymbol{B}}][G_t]\right)^\dagger - \mathbb{I}\right)[G_s]\right](\boldsymbol{\Omega} - \boldsymbol{\Omega}_r). \tag{31}$$

This is equivalent to the system

$$\dot{\boldsymbol{\zeta}} = [A(t)]\boldsymbol{\zeta}, \tag{32}$$

with

$$[A(t)] = -c\left[\mathbb{I} + [G_s]^+\left([\tilde{\boldsymbol{B}}][G_t]\left([\tilde{\boldsymbol{B}}][G_t]\right)^\dagger - \mathbb{I}\right)[G_s]\right] \tag{33}$$

$$\boldsymbol{\zeta} = \boldsymbol{\Omega} - \boldsymbol{\Omega}_r. \tag{34}$$

The time dependency in the $[A(t)]$ matrix is due solely to the variation of the magnetic field. Due to this time dependency, the eigenvalues of the $[A(t)]$ matrix do not sufficiently prove convergence of the wheel speeds to the desired biases. Even if $[A(t)]$ is Hurwitz (all eigenvalues have negative real parts) for all time, there is no guarantee. Furthermore, the dynamic nature of the problem of interest makes it impossible to analytically demonstrate certain properties of the $[A(t)]$ matrix. The magnetic field experienced by the spacecraft is dependent on the spacecraft's position and orientation relative to the earth, and this determines how $[A(t)]$ varies with time. Currently, numerical simulations illustrate the efficacy of the proposed momentum dumping algorithm. Further analysis on the proposed momentum dumping algorithm is left for future work.

NUMERICAL SIMULATION

To demonstrate functionality of the control law and momentum dumping strategy, numerical simulation is used. A scenario is considered where the spacecraft is to track the rotating Hill frame.[3,23] Let the instantaneous orbital position of the spacecraft be denoted as $\boldsymbol{r}$, and its velocity by $\boldsymbol{v}$. The Hill frame is then defined by the unit vectors

$$\hat{\boldsymbol{o}}_r = \frac{\boldsymbol{r}}{|\boldsymbol{r}|}, \quad \hat{\boldsymbol{o}}_\theta = \hat{\boldsymbol{o}}_h \times \hat{\boldsymbol{o}}_r, \quad \hat{\boldsymbol{o}}_h = \frac{\boldsymbol{r}\times\boldsymbol{v}}{|\boldsymbol{r}\times\boldsymbol{v}|}. \tag{35}$$

In this scenario, the goal is to reorient the spacecraft such that $\hat{\boldsymbol{b}}_1 \to \hat{\boldsymbol{o}}_r$, $\hat{\boldsymbol{b}}_2 \to \hat{\boldsymbol{o}}_\theta$, and $\hat{\boldsymbol{b}}_3 \to \hat{\boldsymbol{o}}_h$. The orbital elements used to simulate the orbital motion are given in Table 1. Here, a circular orbit is used, which corresponds to reference angular velocity of

$$\boldsymbol{\omega}_r = n\hat{\boldsymbol{o}}_h, \tag{36}$$

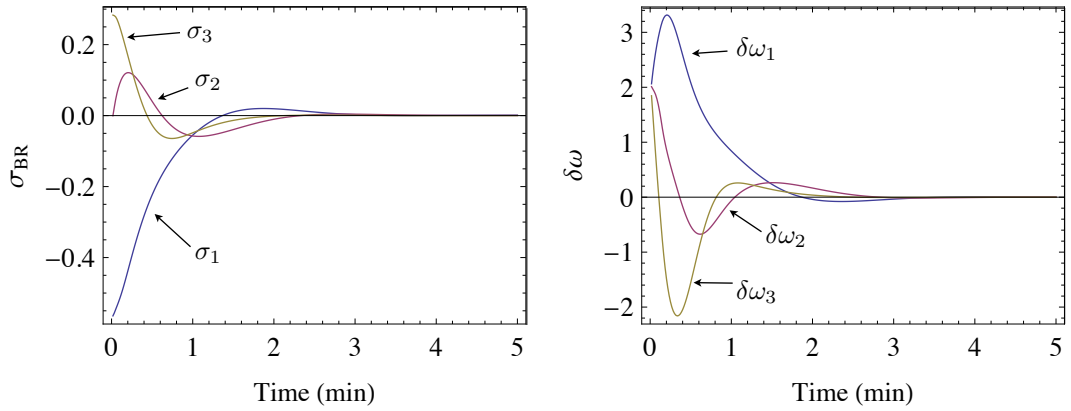

Figure 2. Relative attitude (left) and angular velocity (right) of body frame relative to Hill frame during pointing maneuver

where n is the orbital mean motion. The Hill frame rotates about the $\hat{\boldsymbol{o}}_h$ axis at a rate equal to n. To propagate the orbit, two-body dynamics are used.

In order to simulate magnetic torque bar behavior, a magnetic field model is needed. For this study, the tilted-centered dipole magnetic field model is used, with magnetic field components defined by[16]

$$\begin{bmatrix} B_{North} \\ B_{East} \\ B_{Down} \end{bmatrix} = -\frac{6378\text{km}}{r^3} \begin{bmatrix} -\cos\phi & \sin\phi\cos\lambda & \sin\phi\sin\lambda \\ 0 & \sin\lambda & -\cos\lambda \\ -2\sin\phi & -2\cos\phi\cos\lambda & -2\cos\phi\sin\lambda \end{bmatrix} \begin{bmatrix} 29900 \\ 1900 \\ -5530 \end{bmatrix} nT. \tag{37}$$

Note that in the earth-centered earth fixed (ECEF) frame, the magnetic field is constant. In the earth-centered inertial (ECI) frame, the magnetic field rotates along with the earth. The spacecraft orbit is propagated in the ECI frame, and the rotation of the earth must be modeled. For the simulation, the ECEF and ECI frames are assumed to be aligned initially, and the earth rotates about the z axis at a rate of 7.292×10^{-5} rad/sec.

The spacecraft is assumed to have three magnetic torque bars and four reaction wheels. In the spacecraft body frame, the alignment axes for these devices are

$$[G_t] = \begin{bmatrix} 1 & 0 & 0 \\ 0 & 1 & 0 \\ 0 & 0 & 1 \end{bmatrix}, \quad [G_s] = \begin{bmatrix} 0 & 0 & \cos(45^\circ) & -\cos(45^\circ) \\ \cos(45^\circ) & \sin(45^\circ) & -\sin(45^\circ) & -\sin(45^\circ) \\ \sin(45^\circ) & -\cos(45^\circ) & 0 & 0 \end{bmatrix}.$$

Each reaction wheel is assumed to have the same spin-axis inertia value of $J_{si} = 0.001$ kg m^2 and a maximum torque of 30 mNm. The torque bars are limited to a maximum dipole of 20 Am^2. A diagonal inertia tensor is assumed, with the values

$$[I] = \begin{bmatrix} 10.5 & 0 & 0 \\ 0 & 8 & 0 \\ 0 & 0 & 6.75 \end{bmatrix} \text{kg m}^2.$$

Lastly, the control gains implemented for the numerical simulation are summarized in Table 2.

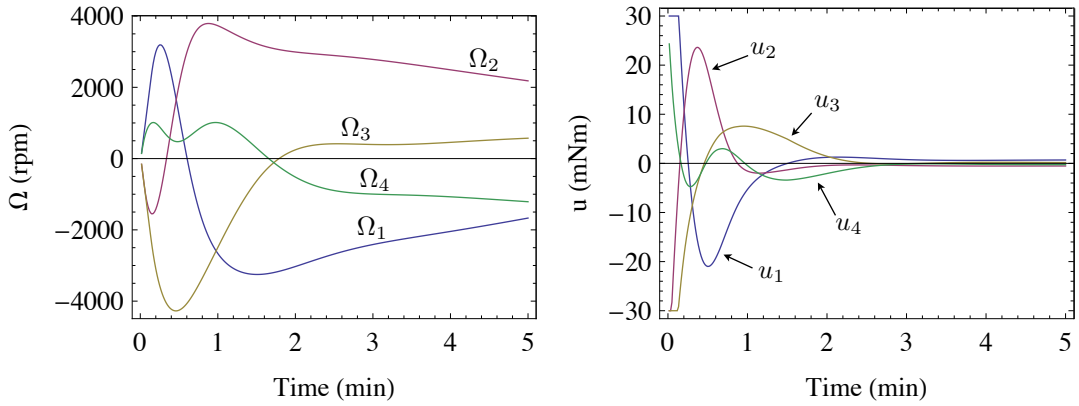

Figure 3. Reaction wheel speeds (left) and motor torques (right) during pointing maneuver

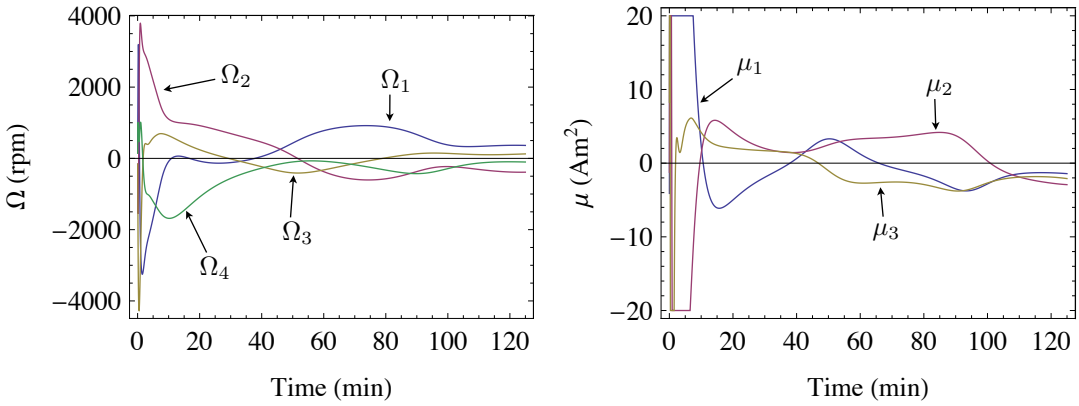

Figure 4. Reaction wheel speeds (left) and torque bar dipoles illustrating continuous momentum dumping during pointing maneuver

The initial conditions used for the simulation are $\boldsymbol{\omega}_0 = \begin{bmatrix} 2.0 & 2.0 & 2.0 \end{bmatrix}^T$ deg/sec, $\boldsymbol{\Omega} = \mathbf{0}$ rad/sec, and $\boldsymbol{\sigma}_0 = \begin{bmatrix} 0.5 & -0.5 & 0.7 \end{bmatrix}^T$. Here, $\boldsymbol{\sigma}_0$ represents the initial attitude of the spacecraft relative to the ECI frame. For the attitude error $\boldsymbol{\sigma}_{BR}$ is used, which represents the rotation between the reference Hill frame and the spacecraft body frame. To simulate unmodeled torques on the spacecraft, a residual dipole of 1 Am^2 is applied to all three body axes of the spacecraft. The performance of the attitude control law (Eq. (15)) is shown in Figure 2 for the first five minutes of the simulation. The control is successful at converging onto the desired reference Hill frame.

The wheel speeds and motor torques during the first five minutes are shown in Figure 3. There is an increase in wheel speeds of several thousand revolutions per minute (rpm) during the initial detumbling period of roughly one minute. This is due to the wheels absorbing the initial spacecraft momentum, reducing the tumble rate in order to converge to the reference Hill frame. In this short time period, there has not been sufficient time for the magnetic torque bars to remove momentum from the system in spite of the fact that the momentum dumping algorithm is run continuously.

To illustrate momentum dumping, the wheel speeds and magnetic torque bar dipoles are shown in Figure 4 for 125 minutes of simulation time. Wheels 1 and 3 are commanded to a desired bias

of $\Omega_r = 250$ rpm, while wheels 2 and 4 are commanded to a desired bias of $\Omega_r = -250$ rpm. Over this longer time period, the success of the momentum dumping strategy is evident. The wheel speeds are greatly reduced, from a level of several thousand rpm to a few hundred. For the first few minutes of the pointing maneuver, the torque bar dipoles are saturated due to the high wheel speeds and aggressive momentum dumping torques called for. As the wheel speeds are reduced, the torque bar commands fall to levels of a few Am^2.

CONCLUSIONS

In this paper, a spacecraft attitude control law is developed for a redundant cluster of reaction wheels. The control law, which includes integral feedback to account for unmodeled torques, is an improvement over similar control strategies previously developed in that it does not contain a term that is quadratic in angular velocity. The issue of momentum dumping is also addressed in the current study. Prior work implements momentum management strategies for non-redundant reaction wheel clusters that have limitations in their application to a spacecraft equipped with 4 or more reaction wheels. A new method of momentum dumping is developed, which does not experience the shortcomings inherent in prior work. Numerical simulation is used to demonstrate the efficacy of the new control scheme, illustrating proper tracking behavior and momentum dumping for the case of a time-varying reference attitude.

REFERENCES

[1] W. H. Steyn, "Near-Minimum-Time Eigenaxis Rotation Maneuvers Using Reaction Wheels," *AIAA Journal of Guidance, Control, and Dynamics*, Vol. 18, Sept. 1995, pp. 1184–1189.

[2] S. B. Skaar and L. G. Kraige, "Large-Angle Spacecraft Attitude Maneuvers Using an Optimal Reaction Wheel Power Criterion," *Journal of the Astronautical Sciences*, Vol. 32, No. 1, 1984, pp. 47–61.

[3] H. Schaub and J. L. Junkins, *Analytical Mechanics of Space Systems*. Reston, VA: AIAA Education Series, 2nd ed., October 2009.

[4] H. Schaub and V. J. Lappas, "Redundant Reaction Wheel Torque Distribution Yielding Instantaneous L_2 Power-Optimal Attitude Control," *AIAA Journal of Guidance, Control, and Dynamics*, Vol. 32, July–Aug. 2009, pp. 1269–1276.

[5] J. R. Glaese, H. F. Kennel, G. S. Nurre, S. M. Seltzer, and H. L. Shelton, "Low-Cost Space Telescope Pointing Control System," *Journal of Spacecraft*, Vol. 13, July 1976, pp. 400–405.

[6] M. A. Karami and F. Sassani, "Spacecraft momentum dumping using less than three external control torques," *Systems, Man and Cybernetics, 2007. ISIC. IEEE International Conference on*, oct. 2007, pp. 4031 –4039.

[7] X. Chen and W. H. Steyn, "Optimal Combined Reaction-Wheel Momentum Management for LEO Earth-Pointing Satellites," *12th AIAA/USU Conference on Small Satellites*, No. SSC98-IX-2, September 1998.

[8] Z. Ismail and R. Varatharajoo, "A study of reaction wheel configurations for a 3-axis satellite attitude control," *Advances in Space Research*, Vol. 45, 2010, pp. 750–759.

[9] Z. Fan, S. Hua, M. Chundi, and L. Yuchang, "An Optimal Attitude Control of Small Satellite with Momentum Wheel and Magnetic Torqrods," *Proceedings of the 4th World Congress on Intelligent Control and Automation*, Shanghai, P.R. China, June 10-14 2002, pp. 1395–1398.

[10] W. H. Steyn, "Comparison of Low-Earth-Orbit Satellite Attitude Controllers Submitted to Controllability Constraints," *Journal of Guidance, Control, and Dynamics*, Vol. 17, July-Aug 1994, pp. 795–804.

[11] G. T. Kroncke and R. P. Fuchsi, "An Algorithm for Magnetically Dumping GPS Satellite Angular Momentum," *Journal of Guidance, Control, and Dynamics*, Vol. 1, No. 4, 1978, pp. 269–272.

[12] T. F. Wiener, *Theoretical Analysis of Gimballess Inertial Reference Equipment Using Delta-Modulated Instruments*. Ph.D. dissertation, Department of Aeronautics and Astronautics, Massachusetts Institute of Technology, Cambridge, MA, March 1962.

[13] M. D. Shuster, "A Survey of Attitude Representations," *Journal of the Astronautical Sciences*, Vol. 41, No. 4, 1993, pp. 439–517.

[14] S. R. Marandi and V. J. Modi, "A Preferred Coordinate System and the Associated Orientation Representation in Attitude Dynamics," *Acta Astronautica*, Vol. 15, No. 11, 1987, pp. 833–843.

[15] H. Schaub and J. L. Junkins, "Stereographic Orientation Parameters for Attitude Dynamics: A Generalization of the Rodrigues Parameters," *Journal of the Astronautical Sciences*, Vol. 44, No. 1, 1996, pp. 1–19.

[16] M. D. Griffin and J. R. French, *Space Vehicle Design*. AIAA Education Series, 2004.

[17] J. L. Crassidis and F. L. Markley, "Sliding mode control using modified Rodrigues parameters," *Journal of Guidance, Control, and Dynamics*, Vol. 19, No. 6, 1996, pp. 1381–1383.

[18] P. Tsiotras, "New Control Laws for the Attitude Stabilization of Rigid Bodies," *13th IFAC Symposium on Automatic Control in Aerospace*, Sept. 12-16 1994, pp. 316–321.

[19] H. Schaub, R. D. Robinett, and J. L. Junkins, "Globally Stable Feedback Laws for Near-Minimum-Fuel and Near-Minimum-Time Pointing Maneuvers for a Landmark-Tracking Spacecraft," *Journal of the Astronautical Sciences*, Vol. 44, No. 4, 1996, pp. 443–466.

[20] S. Krishnan and S. R. Vadali, "An Inverse-Free Technique for Attitude Control of Spacecraft Using CMGs," *Acta Astronautica*, Vol. 39, No. 6, 1997, pp. 431–438.

[21] R. Mukherjee and D. Chen, "Asymptotic Stability Theorem for Autonomous Systems," *Journal of Guidance, Control, and Dynamics*, Vol. 16, 1993, pp. 961–963.

[22] A. Ben-Israel and T. N. Greville, *Generalized Inverses: Theory and Applications*. Springer, 2003.

[23] W. H. Clohessy and R. S. Wiltshire, "Terminal Guidance System for Satellite Rendezvous," *Journal of the Aerospace Sciences*, Vol. 27, No. 9, 1960, pp. 653–658.